Stereochemistry of the Enolization of Scytalone by Scytalone Dehydratase

Douglas B. Jordan,‡ Ya-Jun Zheng,‡ Bruce A. Lockett,‡ and Gregory S. Basarab*,§

Stine-Haskell Research Center, E. I. DuPont de Nemours Agricultural Products, P.O. Box 30, Newark, Delaware 19714, and Biochemical Sciences and Engineering, E. I. DuPont de Nemours Central Research and Development, P.O. Box 80328, Experimental Station, Wilmington, Delaware 19880-0328

Received August 6, 1999; Revised Manuscript Received December 14, 1999

ABSTRACT: In D_2O, scytalone exchanges its two C2 hydrogen atoms for deuterium atoms at different rates. At pD 7.0 and 25 °C, half-lives for the exchanges are 0.8 and 10 days for the *pro-S* and *pro-R* hydrogens, respectively. The differential exchange rates allow for the preparation of multiple scytalone samples (through incubation of scytalone in D_2O and then back exchanging with H_2O) having differential levels of deuterium enrichment at the C2 *pro-S* and *pro-R* positions. From these samples, the stereochemical preference for hydrogen abstraction during the dehydration reaction mediated by the enzyme scytalone dehydratase was determined. At pH 7.0, deuterium at the *pro-S* position has little effect on enzyme catalysis, whereas deuterium at the *pro-R* position produces kinetic isotope effects of 2.3 (25 °C), 5.1 (25 °C), and 6.7 (6.8 °C) on k_{cat}, k_{cat}/K_m, and the single-turnover rate, respectively. The results are fully consistent with the enzyme catalyzing a *syn* elimination through an E1cb-like mechanism. The *syn* elimination is compatible with the interactions realized between a scytalone boat conformation and key active site residues as modeled from multiple X-ray crystal structures of the enzyme in complexes with inhibitors.

Scytalone dehydratase (SD,[1] EC 4.2.1.94) efficiently catalyzes the dehydrations of scytalone and vermelone, two intermediates within the fungal melanin biosynthetic pathway (*1*−*7*). The enzyme is the target of new fungicides (*8*−*10*) that are useful for controlling rice blast, a perennial disease that is responsible for extensive losses in grain yields (*11*). Numerous X-ray crystal structures of SD have been exploited through structure-based design and synthesis programs to generate SD inhibitors having picomolar binding constants, several of which provide excellent control of blast disease (*12*−*14*). The mechanism of the enzyme-catalyzed dehydration of scytalone is considered highly pertinent to the understanding of inhibitor binding, particularly in view of the noted mimics of the enol intermediate of scytalone displayed by potent inhibitors (*15*) and the noted participation of catalytic residues for inhibitor binding (*16*, *17*). Gerlt and Gassman recognized that an efficient enzyme must offer an environment that can lower the acidity α to carbonyls to account for catalysis (*18*−*21*). They proposed that an E1cb-like mechanism might be common in enzyme-catalyzed dehydrations wherein the enzyme protonates the carbonyl to induce enolization. Corey and Sneen first proposed the importance of stereoelectronic effects in enolization of carbonyls in 1956 (*22*), and such effects must certainly apply to the enolization of scytalone. The majority of dehydratase enzymes that have been studied operate on acyclic substrates for which the stereochemical course for removal of the elements of water can be either *syn* or *anti* (*23*). The saturated ring of scytalone constrains the conformational flexibility of the carbon atoms bearing the elements of water, lowering the entropic penalty for achieving the *syn* and *anti* orientations.

Scheme 1: Dehydration of Scytalone to Trihydroxynaphthalene

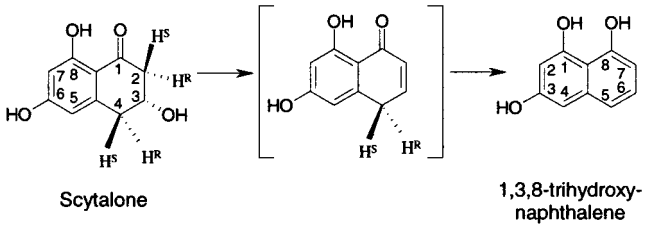

SD facilitates a 1 billion-fold enhancement in the scytalone dehydration rate in comparison to the non-enzyme-catalyzed rate in aqueous medium at neutral pH and 25 °C (*17*). Kinetic analysis of wild-type SD and a series of site-directed mutants suggests that the enzyme binds substrate and catalyzes a *syn* elimination via the action of two tyrosine residues, two histidine residues, an asparagine residue, and a serine residue. As proposed, tyrosines 30 and 50 (phenolic hydroxyls) assist in the acidification of an active-site water molecule that promotes enolization of scytalone in concert with the abstraction of the hydrogen from the C2 position mediated by the imidazole of His85 (*16*, *17*). Immediately afterward, hydroxide elimination (from C3) is assisted by proton donation from the (then) protonated imidazole of His85 and by hydrogen bonding of the C3 hydroxyl hydrogen with the imidazole of His110. Tautomerization to generate 1,3,8-trihydroxynaphthalene (3HN) completes the catalytic cycle (Scheme 1). Thus, the enzyme-catalyzed dehydration is believed to proceed in the two sequential steps as defined

* To whom correspondence should be addressed: Biochemical Sciences and Engineering, E. I. DuPont de Nemours Central Research and Development, P.O. Box 80328, Experimental Station, Wilmington, DE 19880-0328. Telephone: (302) 695-4510. Fax: (302) 695-3786. E-mail: gregory.s.basarab@usa.dupont.com.

‡ E. I. DuPont de Nemours Agricultural Products.

§ E. I. DuPont de Nemours Central Research and Development.

[1] Abbreviations: SD, scytalone dehydratase; DMSO, dimethyl sulfoxide; E1cb, elimination first-order conjugate base; KIE, kinetic isotope effect.

10.1021/bi991839y CCC: $19.00
Published on Web 02/08/2000

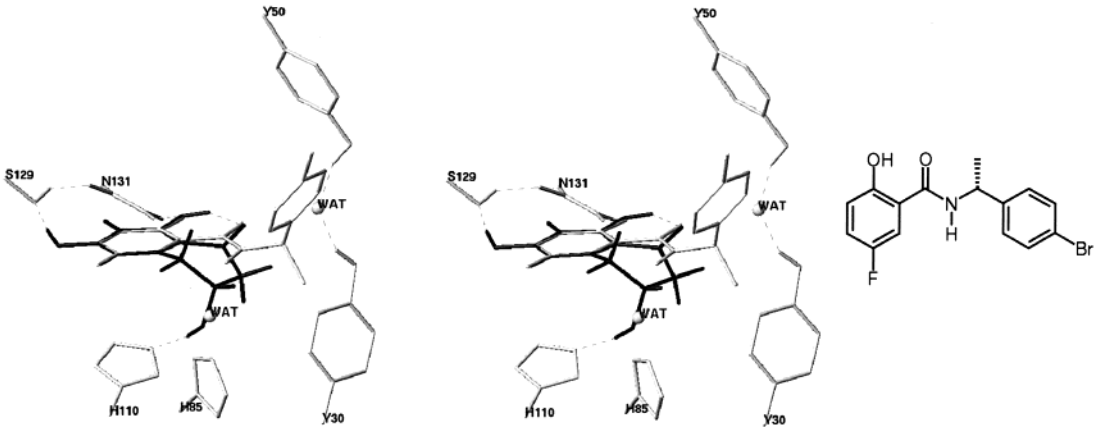

FIGURE 1: Stereoview of scytalone in the SD active site. The scytalone boat conformation was overlayed on the inhibitor (structure to the right) in a model of the complex with SD as determined by X-ray crystallography [PDB entry 3STD (*15*)]. Hydrogen bonds are represented by dashed lines. Two water molecules are shown as spheres with one mapping close to the leaving hydroxyl of scytalone.

by an E1cb-like mechanism, though the kinetic data suggest that the activation barriers for each of the individual steps are similar. Molecular orbital theory calculations support the idea that acid catalysis by the two tyrosine residues in concert with a bound water molecule induces enol formation in the transition state for the dehydration (*24*). It has been shown that having the two tyrosine residues assist in donating a proton through the water molecule increases SD's catalytic efficiency by about 10-fold (*17*). Active site recognition of the productive conformation of scytalone is achieved via the side chains of Asn129 and Ser131 along with the catalytic side chains of His85, His110, Tyr30, and Tyr50 (*15*, *17*). Alanine and threonine mutations of Ser129 were critical for securing the orientation of the C6 hydroxyl of scytalone (toward the Ser129 side chain hydroxyl) for sharing a hydrogen bond, thereby validating a model of scytalone within the SD active site (*17*). To carry out a *syn* elimination, it was proposed that scytalone adopts a boat conformation with the C3 hydroxyl and the C2 *pro-R* hydrogen in axial orientations.

The proposed mechanism outlined above largely depends on inferences from a model of scytalone docked in the active site of SD in place of a salicylamide inhibitor (Figure 1). However, there is no direct evidence implicating a *syn* elimination. Furthermore, there is the possibility that the larger size of the inhibitor relative to the substrate distorts the active site in a way that invalidates the model. We set out to determine conclusively SD's stereochemical preference for hydrogen abstraction at the C2 position of scytalone. In principle, this preference could be determined by running the enzyme-catalyzed reaction in reverse with 3HN deuterated at C7 so that the labeled scytalone that is produced could be recovered and analyzed. In practice, there are considerable barriers to performing such an experiment. The equilibrium constant for the scytalone−3HN couple lies at least 200-fold in favor of 3HN; the C7 hydrogen of 3HN exchanges with aqueous solvent, and 3HN is unstable, being subject to oxidation and self-polymerization reactions. In a more practical approach to the problem, we sought evidence supporting an enol intermediate in the enzyme-catalyzed dehydration of scytalone by analysis of the C2 position of scytalone when it was incubated with the enzyme in D_2O during partial conversion to product (*17*). However, there is a strong commitment to hydroxide elimination upon enolization of scytalone in the enzyme-catalyzed dehydration reaction, preventing the incorporation of deuterium at C2 and precluding the determination of the stereochemical outcome. An unambiguous and simple experimental solution to the stereospecificity question is reported in this work. Namely, the findings reported here are that the C2 *pro-R* and *pro-S* positions of scytalone can be differentially enriched with deuterium in stable preparations and that, by measuring the kinetic isotope effect (KIE) of these scytalone samples on SD catalysis, the selectivity for C2 hydrogen removal during catalysis can be ascertained.

EXPERIMENTAL PROCEDURES

Materials and General Methods. Homogeneous SD was purified as described previously (*4*). Scytalone was purified from cultures of *rsy*$^-$ mutants of *Magnaporthe grisea* (*3*). ^{1}H NMR spectra were recorded on a Varian VXR-400-ND spectrometer. Spectra of scytalone samples in aqueous incubation medium [H_2O and 100 mM sodium phosphate (pH 7.0)] were recorded using the wet1d pulse sequence (with a pulse angle of 87° and an interscan delay of 20 s), which allowed suppression of the water resonance. NOE enhancements were measured from the ^{1}H NMR of scytalone recorded in d_6-DMSO with preirradiation of each of the resonances for 10 s.

Determination of Kinetic Isotope Effects (KIEs). Steady-state kinetic constants were determined at pH 7.0 (100 mM sodium phosphate) and 25 °C as described previously (*6*, *15*, *17*). Initial rate data were fitted to eq 1.

$$v = \frac{k_{cat}A}{A + K} \quad (1)$$

where k_{cat} is the maximum velocity, K is the Michaelis constant, A is the varied substrate concentration, and v is the observed velocity (*25*). Single-turnover measurements were conducted using a stopped-flow instrument (Applied Photophysics, Leatherhead, U.K.) essentially as described previously (*17*). Reaction mixtures (0.1 s) contained 100 mM sodium phosphate, 25 μM scytalone sample, and 100 μM SD at pH 7.0 and 6.8 °C; absorbency data (352 nm) were fitted to a single-exponential equation. KIEs for the single-turnover rate constants were corrected for deuterium enrichment through eq 2 (*26*)

$$^{D}k = \frac{k_H(\text{obs})F}{k_D(\text{obs}) - k_H(\text{obs})(1 - F)} \quad (2)$$

where ^{D}k is the corrected KIE, k_H(obs) is the observed rate with the proteo substrate, k_D(obs) is the observed rate with the partially deuterated substrate, and F is the fraction of deuterium enrichment at the respective C2 positions of scytalone.

Transformation of eq 2 to the linear form of eq 3 was used for fitting kinetic data from multiple scytalone samples partially enriched in deuterium.

$$k_D(\text{obs}) = \left[\frac{k_H(\text{obs})}{^{D}k} - k_H(\text{obs})\right]F + k_H(\text{obs}) \quad (3)$$

Deuterium Exchange into Scytalone. Scytalone (40 mg) was dissolved in 10 mL of D_2O buffered to pD 7.0 with 100 mM sodium phosphate. A 1 mL aliquot was removed for NMR analysis. NMR spectra were recorded from this sample at 20 min, 6 h, and daily for the following 14 days. The solution was maintained at 25 °C. Aliquots (2 mL) of the D_2O solution of scytalone were removed after 2.3, 4.3, and 60 days and stored at −80 °C for later purification and analysis. Each of the 2.3, 4.3, and 60 day aliquots was extracted three times with ethyl acetate, dried ($MgSO_4$), and concentrated. The residues were chromatographed on silica gel (ether) to give 9.7, 9.5, and 8.9 mg, respectively, of differentially deuterated scytalone for the 2.3, 4.3, and 60 day samples. ^{1}H NMR (d_6-acetone) for the 2.3 day sample: δ 12.8 (s, 1H), 9.4 (s, 1H), 6.3 (s, 1H), 6.2 (s, 0.6H), 4.3 (s, 2H), 3.1 (dd, J = 16, 3 Hz, 1H), 2.8−2.95 (m, obscured by HOD), 2.5 (d, J = 9 Hz, 0.7 H). ^{1}H NMR (d_6-acetone) for the 4.3 day sample: δ 12.8 (s, 1H), 9.4 (s, 1H), 6.3 (s, 1H), 6.2 (s, 0.5H), 4.3 (s, 2H), 3.1 (dd, J = 16, 3 Hz, 1H), 2.8−2.95 (m, obscured by HOD), 2.5 (d, J = 9 Hz, 0.6 H). ^{1}H NMR (d_6-acetone) for the 60 day sample: δ 12.8 (s, 1H), 9.4 (s, 1H), 6.3 (s, 0.7H), 6.2 (s, 0.09H), 4.3 (s, 2H), 3.1 (dd, J = 16, 3 Hz, 1H), 2.8−2.95 (m, obscured by HOD), 2.5 (m, 0.09 H). ^{1}H NMR (d_6-DMSO) for the 2.3 day sample: δ 12.7 (s, 1H), 10.6 (s, 1H), 6.2 (s, 1H), 6.1 (s, 0.6H), 5.1 (d, J = 4 Hz, 1H), 4.15 (m, 1H), 3.0 (dd, J = 16, 3 Hz, 1H), 2.75 (dd, J = 17, 7 Hz, 1.3H), 2.5 (obscured by proteo DMSO). ^{1}H NMR (d_6-DMSO) for the 4.3 day sample: δ 12.7 (s, 1H), 10.6 (s, 1H), 6.2 (s, 1H), 6.1 (s, 0.5H), 5.1 (d, J = 4 Hz, 1H), 4.15 (m, 1H), 3.0 (dd, J = 16, 3 Hz, 1H), 2.75 (dd, J = 17, 7 Hz, 1.1H), 2.5 (obscured by proteo DMSO). ^{1}H NMR (d_6-DMSO) for the 60 day sample: δ 12.7 (s, 1H), 10.6 (s, 1H), 6.2 (s, 0.6H), 6.1 (s, 0.09H), 5.1 (d, J = 4 Hz, 1H), 4.15 (m, 1H), 3.0 (dd, J = 16, 3 Hz, 1H), 2.75 (dd, J = 17, 7 Hz, 1.06 H), 2.5 (obscured by proteo DMSO). ^{1}H NMR (D_2O, 20 min): δ 6.3 (d, J = 2 Hz, 1H), 6.1 (d, J = 2 Hz, 1H), 4.15 (m, 1H), 3.1 (dd, J = 16, 3 Hz, 1H), 2.95 (dd, J = 17, 4 Hz, 1H), 2.9 (dd, J = 16, 7 Hz, 1H), 2.65 (ddd, J = 17, 7, 1 Hz).

Hydrogen Exchange into Deuterated Scytalone. Scytalone (6 mg) from the 60 day D_2O incubation was dissolved in 4 mL of H_2O buffered to pH 7.0 with 100 mM sodium phosphate. A 1 mL aliquot was removed for NMR analysis. NMR spectra were recorded in the H_2O solvent every 2 h for 6 days, and then after 9 and 14 days. The solution was maintained at 25 °C. After 9 and 14 days, 2 mL aliquots were stored at −80 °C for later purification and analysis. Each aliquot was extracted three times with ethyl acetate, dried ($MgSO_4$), and concentrated. The residues were chromatographed though silica gel (ether) to give 2.1 and 1.5 mg, respectively, of differentially deuterated scytalone for the 9 and 14 day samples. ^{1}H NMR (D_2O) for the 9 day sample: δ 6.4 (s, 0.7H), 6.3 (s, 0.7H), 4.4 (s, 1H), 3.1 (dd, J = 16, 4 Hz, 1H), 2.9−3.0 (m, 1.6 H), 2.7 (dd, J = 17, 8 Hz, 0.3H). ^{1}H NMR (D_2O) for the 14 day sample: δ 6.4 (s, 0.8H), 6.3 (s, 0.8H), 4.4 (s, 1H), 3.1 (dd, J = 16, 4 Hz, 1H), 2.9−3.0 (m, 1.7 H), 2.7 (dd, J = 17, 8 Hz, 0.3H).

RESULTS

Stereochemistry of Deuterium Incorporation into Scytalone. The coupling constants for scytalone from the NMR spectra in D_2O and d_6-DMSO are nearly identical, indicating that the conformations adopted by scytalone in the two solvents are quite similar. NOE experiments were therefore carried out in d_6-DMSO to avoid the exchange of hydrogens that occurs in D_2O. The NOE enhancements seen for the resonances at 2.85−2.9 and 3.08−3.15 ppm on preirradiation of the C5 hydrogen at δ 6.2 positively assign them to the C4 hydrogens, leaving the resonances at 2.5−2.75 and 2.9−2.95 ppm to be assigned to the C2 position. Preirradiation of the signal generated by the C3 carbinol hydrogen expresses a much greater NOE enhancement for the C2 and C4 hydrogens *anti* to the hydroxyl than for the corresponding *syn* hydrogens, thereby establishing the stereochemistry of the *anti* hydrogens as *pro-S* and the *syn* hydrogens as *pro-R*. Saturation of the signal corresponding to the C3 hydroxyl hydrogen produced an NOE only for the two hydrogens at C2 and C4 *syn* to the hydroxyl. Scytalone can be expected to undergo rapid conformational interconversion, but the chiral center at C3 would predispose the hydrogen atoms on the same side of the scytalone saturated ring to being positioned spatially closer to one another most of the time.

In D_2O, the downfield C2 hydrogen (*pro-S*) exchanges for deuterium 13-fold more rapidly than the upfield resonance reflecting the *pro-R* hydrogen (Figure 2A). Half-lives for the exchanges are 0.79 ± 0.04 and 10 ± 0.7 days^{-1} for the *pro-R* and *pro-S* hydrogens, respectively. The *pro-S* hydrogen exchanges for deuterium at a rate 86 times faster than the dehydration rate, while the *pro-R* hydrogen exchanges at a rate 6.6 times faster than the dehydration rate. Deviations in the exchange data from a simple exponential decay can be attributed to the complexity introduced by the secondary isotope effect due to deuterium exchange with time for the alternate C2 hydrogen. Figure 3 shows the scytalone NMR spectra in D_2O between 2.3 and 3.5 ppm after incubation in D_2O for 20 min and 15 days. The resonance at 2.85−2.9 ppm is lost with the longer incubation time, while the 2.6−2.75 ppm resonance collapses to a doublet (J = 6 Hz) while diminishing in intensity. Also observed is the slow exchange of the C7 and C5 aromatic hydrogen atoms during the incubation in D_2O with half-lives of 8.5 and 140 days, respectively. Neither of these hydrogen atoms is expected to influence the kinetics of the dehydration on the enzyme as they are well removed from the chemical events.

Scytalone (94% deuterium in both the C2 *pro-R* and *pro-S* positions) incubated in D_2O for 60 days was purified and then incubated in H_2O [100 mM sodium phosphate (pH 7.0)] at 25 °C. Its hydrogen content was determined for 14 days

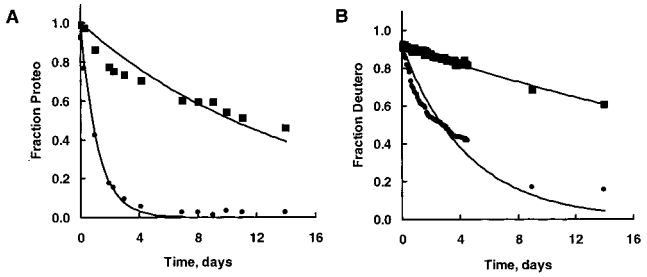

FIGURE 2: Exchange of the C2 hydrogens and deuteriums of scytalone with aqueous solvent. (A) Exchange rates of the C2 *pro-R* and *pro-S* hydrogens of all-proteo scytalone for deuteriums upon incubation in D_2O [100 mM sodium phosphate (pD 7.0)] at 25 °C. The fractions of hydrogens remaining vs time are indicated for the *pro-R* (■) and *pro-S* positions (●) at C2 of scytalone on the basis of NMR analyses. The calculated rates for exchange at the respective positions are represented by the curves, which were fitted to a single-exponential equation having a *Y*-intercept of 1 and a *X*-intercept of 0. The fitted rate of exchange for the *pro-R* position is 0.067 ± 0.005 day^{-1}. The fitted rate of exchange for the *pro-S* position is 0.87 ± 0.04 day^{-1}. (B) Exchange rates of the C2 *pro-R* and *pro-S* deuterons of deuterated scytalone (94% deuterated at both C2 positions) for hydrogens upon incubation in H_2O [100 mM sodium phosphate (pH 7.0)] at 25 °C. The fractions of deuterons remaining vs time are indicated for the *pro-R* (■) and *pro-S* positions (●) at C2 of scytalone. The calculated rates for exchange at the respective positions are represented by the curves, which were fitted to a single-exponential equation having a *Y*-intercept of 0.94 and a *X*-intercept of 0. The fitted rate of exchange for the *pro-R* position is 0.030 ± 0.0006 day^{-1}. The fitted rate of exchange for the *pro-S* position is 0.220 ± 0.006 day^{-1}.

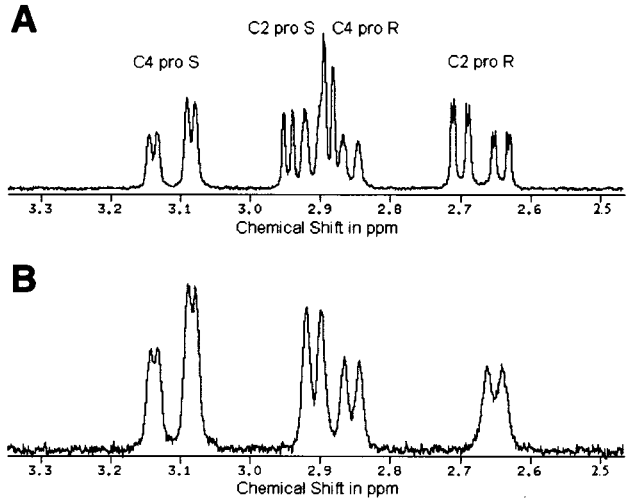

FIGURE 3: NMR traces for the region between 2.3 and 3.5 ppm for scytalone in D_2O: (A) after 20 min and (B) after 14 days.

by ^{1}H NMR (Figure 2B). The rates of exchange of the C2 deuteriums for hydrogens are slower than the corresponding rates measured for the all-proteo scytalone incubated in D_2O: 2.2-fold slower for the *pro-R* position and 4.0-fold slower for the *pro-S* position. Full deuterium isotope effects for this back exchange are not measured, in part, due to the depletion of substrate through dehydration.

Scytalone on the Enzyme. The finding that the two C2 position hydrogens have significantly different rates for deuterium exchange allows for the preparation of scytalone samples with varying deuterium content depending on the incubation times in D_2O. Scytalone (20 mM) in 100 mM sodium phosphate (pD 7.0) was incubated at 25 °C, and samples were removed after 2.3, 4.3, and 60 days (as described for Figure 2A) and stored at −80 °C. The samples were purified and analyzed by ^{1}H NMR (Table 1). NMR spectra were collected in both d_6-DMSO and d_6-acetone as the signal from proteo DMSO overlapped the resonance from the scytalone *pro-R* hydrogen while the HOD impurity of d_6-acetone overlapped the resonance from the *pro-S* hydrogen. The estimated deuterium enrichments at the C2 *pro-R* position of scytalone equaled 35, 44, and 94% for the D_2O samples of scytalone incubated for 2.3, 4.3, and 60 days, respectively; corresponding deuterium enrichments at the C2 *pro-S* position equaled 85, 90, and 94%, respectively. Deviations from the expected enrichments may be attributed, in part, to the limits of ^{1}H NMR analysis. With longer incubation times (60 day), the deviation from expectation is attributed to adventitious contamination of the D_2O solvent with H_2O. In addition, purification of the samples on silica gel led to some deterioration of the deuterium content of both the *pro-R* and *pro-S* hydrogens.

Scytalone samples with greater deuterium enrichments at the *pro-R* position than at the *pro-S* position were prepared from the scytalone sample incubated in D_2O for 60 days (containing 94% deuterium at both C2 positions) by incubation in H_2O [100 mM sodium phosphate (pH 7.0) at 25 °C] for 9 and 14 days. The two samples were purified; the deuterium contents at the *pro-R* position were 68 and 60%, respectively, and the corresponding deuterium contents at the *pro-S* position were 17 and 15%, respectively.

The enzyme kinetic parameters determined using the five partially deuterated scytalone samples and the all-proteo scytalone are presented in Table 1. For the sample containing 94% deuterium at both the *pro-R* and *pro-S* positions, the corrected deuterium KIE values equal 2.3 (25 °C), 5.1 (25 °C), and 6.7 (6.8 °C) for k_{cat}, k_{cat}/K_m, and the single-turnover rate, respectively. The smaller KIE on k_{cat} in comparison to the KIEs measured for k_{cat}/K_m and the single-turnover rate is attributed to a slow step occurring after the first irreversible step in the enzyme-catalyzed reaction as was similarly observed for d_6-scytalone (2,2,4,4,5,7-hexadeuterioscytalone) (*17*). We believe the slow step reflects the aromatization of the dehydrated scytalone from the enone as depicted in Scheme 1 (*17*).

Enzyme rates are sensitive to deuterium at the C2 *pro-R* position but not at the *pro-S* position as seen from the strong correlation for the measured kinetic parameters with the deuterium content of the former and not the latter (Figure 4A,B). The linear regressions in panels A and B of Figure 4 reflect the theoretical relative velocities from single-turnover experiments assuming a deuterium KIE of 6.7 on the single-turnover rate. Fitting the single-turnover data from Table 1 to eq 3 affords KIE values of 7.8 ± 0.6 when basing the *F* values (the fraction of deuterium content) on the deuterium enrichments at the C2 *pro-R* position; the KIE is 1.3 ± 1.8 when the deuterium enrichments at the C2 *pro-S* position are fitted to eq 3.

DISCUSSION

Stereochemistry of the SD-Catalyzed Dehydration. For efficient catalysis, SD must engineer three adaptations. First, it must select or induce the conformation of scytalone that orients one of the C2 hydrogen atoms and the leaving hydroxyl into axial positions. Second, it must lower the activation energy for enolization by raising the acidity at C2

Table 1: Characteristics of Deuterium-Labeled Scytalone Samples[a]

time in D_2O (days)	0	2.3	4.5	60	60	60
time in H_2O (days)	0	0	0	0	9	14
% D *pro-R*[b]	0	35	44	94	68	60
% D *pro-S*[b]	0	85	90	94	17	15
k_{cat} (s^{-1})	73 ± 4	76 ± 3	59 ± 2	34 ± 2	43 ± 2	42 ± 2
k_{cat}/K_m (μM^{-1} s^{-1})	2.7 ± 0.4	2.1 ± 0.2	2.1 ± 0.1	0.56 ± 0.04	1.2 ± 0.08	0.99 ± 0.06
K_m (μM)	27 ± 5	36 ± 4	28 ± 2	60 ± 7	37 ± 4	43 ± 4
single-turnover rate (s^{-1})	160 ± 3	120 ± 3	94 ± 3	32 ± 3	69 ± 8	66 ± 7

[a] Scytalone was incubated in D_2O [100 mM sodium phosphate (pD 7.0)] for the indicated times. Two samples were incubated in D_2O for 60 days, and following isolation, they were incubated in H_2O [100 mM sodium phosphate (pH 7.0)] for the indicated times. [b] Deuterium enrichments were estimated by NMR.

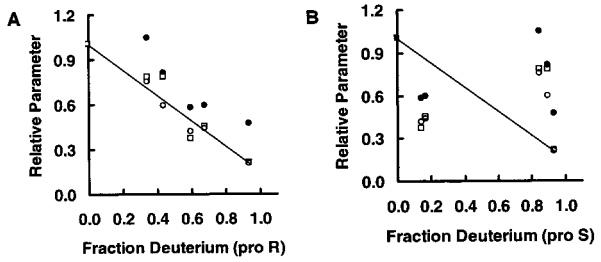

FIGURE 4: Influence of deuterium enrichments in the C2 *pro-R* and *pro-S* positions of scytalone on the kinetic parameters of scytalone dehydratase. The kinetic parameters with respect to the all-proteo scytalone were calculated from those listed in Table 1: k_{cat} (●), k_{cat}/K_m (□), and single-turnover rate (○). For reference, the linear regressions assume a deuterium KIE of 6.7 on the single-turnover rate. (A) Deuterium enrichments in the C2 *pro-R* position of scytalone. (B) Deuterium enrichments in the C2 *pro-S* position of scytalone.

and by positioning a base in the proximity of the axially oriented hydrogen. SD speeds the enolization half-reaction of the dehydration by (4.3×10^7)-fold, if we may compare the rate of solvolytic enolization (removal of the *pro-S* hydrogen) to the enzyme-catalyzed dehydration rate (single-turnover rate). Third, SD must lower the activation energy for the loss of hydroxide by neutralizing the incipient charge. SD speeds this half-reaction by (3.7×10^9)-fold when the solvolytic dehydration rate is compared to the SD-catalyzed single-turnover rate. The measured KIEs on the enzyme kinetic parameters combine the effects of numerous events. In the simplest case, the KIE on the single-turnover rate includes a primary isotope effect on the removal of hydrogen, a secondary isotope effect, and the half-reaction involving the loss of hydroxide. The secondary KIE can be expected to be small. The loss of hydroxide must occur with an energy of activation no greater than that for enolization to account for the expression of the large KIE, which contrasts with the results in the solvolytic dehydration where the KIE is only 1.2 (*17*). Overall, the size of the KIE (6.7) for the single-turnover rate shows that the dehydration rate is dominated by enolization over the loss of hydroxide. A caveat to this interpretation is the possibility that the C2 hydrogen that is removed does not exchange with solvent before delivery to neutralize the leaving hydroxide. Previously, we reported that the C2 hydrogen does not exchange with solvent during catalysis by SD as there is no deuterium incorporation into scytalone during incomplete conversion to product (*17*). Indeed, if the C2 hydrogen that is removed is highly committed to protonating the leaving hydroxide, then the observed KIE would reflect a contribution to raising the energy of activation for the loss of hydroxide in addition to that of deprotonation.

The fact that SD selects the C2 *pro-R* hydrogen of scytalone for removal is crucial to understanding SD catalysis. This preference differs from the dehydration of scytalone off the enzyme where the *pro-S* hydrogen of scytalone is exchanged more rapidly than the *pro-R*. The enzyme reaction has a greater commitment to elimination after enolization (as compared to off the enzyme in aqueous solution), according to the isotope effect results reported here. The X-ray crystal structures of SD in complexes with inhibitors support the conformation of scytalone as shown in Figure 1 as they all have the imidazole of His85 positioned close to the C2 *pro-R* hydrogen to serve as a general base. The inhibitors in the X-ray structures have two sp2 centers in amide or amide-like moieties that were designed to mimic the two sp2 centers of the enol transition state of the SD-catalyzed dehydration reaction (*15*, *17*). These inhibitors have considerably more molecular bulk than the substrate scytalone, and considerable topographical differences in the active site residues may exist between the inhibitor and substrate complexes with the enzyme. In fact, the *syn* elimination established by the deuterium isotope effects corroborates the prediction from modeling scytalone in place of inhibitors within the crystal structures. This *syn* elimination was also supported by site-directed mutagenesis studies of His85, where the mutation to asparagine nearly destroys catalysis (*17*). Hanson and Rose suggested that a single residue could carry out sequential general base−general acid chemistry to promote *syn* eliminations (*27*), much as we propose for SD catalysis. The role of the SD His85−Asp31 dyad in removal of the *pro-R* hydrogen is analogous to that ascribed to the His285−Asp258 dyad for the deprotonation half-reaction of D-galactonate dehydratase (*28*).

The experimentally assigned stereochemical preference for hydrogen abstraction from the C2 position of scytalone places constraints on the conformation of scytalone in the active site. The conformation of scytalone as shown in Figure 1 may be considered to approximate the near attack conformation (NAC) for efficient dehydration. NACs are a focus of a number of studies on explaining the efficiencies of enzyme catalysis (*29*−*35*). The boat conformation minimizes the motions needed not only for hydrogen removal but also for subsequent delivery of the hydrogen to neutralize the leaving hydroxide at C3 because of the proximity of His85 to the axial C2 *pro-R* hydrogen and the axial C3 hydroxyl. The barrier required to achieve the boat conformation is 6.7 kcal/mol (from ab initio calculations; Y.-J. Zheng, unpublished results) with the C2 *pro-R* hydrogen eclipsing the C3 hydroxyl. A slight twist in the boat conformation diminishes the full penalty of the eclipsing interaction, and it is likely that the reaction coordinate proceeds through such a twist-

boat conformation. The kinetics do not exclude the possibility that the C3 hydroxyl is not in an axial or near-axial orientation before hydrogen abstraction with there being a subsequent conformational flip of intermediate enol forms of scytalone. In this scenario, His85 removes the *pro-R* hydrogen from the scytalone envelope conformation with the hydroxyl equatorial. However, by application of principles of least motions as has been done for a variety of organic and biochemical reactions (*36*−*38*), minimizing the conformational changes in both the substrate and enzyme leads to our preference for selection of the boat conformation in Figure 1 as relevant to SD catalysis.

There are energy penalties in the SD-catalyzed reaction for selecting a minority (twist-boat) conformation from the aqueous solution. Consistent with the enzyme kinetic analyses, the X-ray structures of SD show the active site to be poised and apparently fixed to accept this minority boat conformer. Most telling is the imidazole of His110, which is important to catalysis (*17*) and which can enter into a hydrogen bond with the C3 hydroxyl only if the latter is in an axial orientation from the models of scytalone in the active site. With the exception of Tyr50, the residues that are important for catalysis in the SD active site reside on secondary structural elements (α-helices and β-sheets) of the enzyme that do not exhibit significant conformational flexibility (*14*, *15*).

It is worth comparing the results herein with those for the two biochemically distinct types of dehydroquinase, which are well-studied enzymes that also carry out the dehydration of a ring β-hydroxyketone (*39*−*41*). The type I dehydroquinase shares with SD the stereochemical course of a *syn* elimination. However, the 3-dehydroquinate ketone forms an imine with the ϵ-nitrogen of a lysine residue to promote enolization, while SD promotes enolization by protonation of the carbonyl via the complex of a water molecule and the hydroxyl groups of two tyrosine residues. The type II dehydroquinase, like SD, uses no cofactor, metal ion, or lysine residue to carry out catalysis. Unlike SD, it mediates an *anti* elimination, and an arginine residue has been implicated in catalysis. Thus, SD must be viewed as being a catalyst that is distinct from the two dehydroquinases as well as being distinct from a variety of enzymes that catalyze dehydrations of acyclic substrates.

Conclusions. The C2 *pro-R* hydrogen is preferentially removed in the transition state of the enzyme-catalyzed dehydration of scytalone. This is in accord with the previous suggestion that the SD active site residues are poised to accept the diaxial, near attack boat conformation of the substrate for a *syn* elimination. By this model, SD displays the important His85 imidazole for removing the *pro-R* C2 hydrogen and transferring it to the leaving C3 hydroxyl in an E1cb-like mechanism with a single residue functioning as a general base and a general acid.

ACKNOWLEDGMENT

We thank Gina Blankenship, David Clark, Troy C. Gehret, and Rand S. Schwartz for useful discussions and technical expertise.

SUPPORTING INFORMATION AVAILABLE

^{1}H NMR spectra of scytalone in DMSO and incubated in D_2O for 0, 15, and 60 days, ^{1}H NMR spectra of scytalone in H_2O and incubated in D_2O for 60 days followed by 9 and 14 days in H_2O, and ^{1}H NMR NOE spectra of scytalone in DMSO with preirradiation of each of the resonances. This material is available free of charge via the Internet at http://pubs.acs.org.

REFERENCES

1. Bell, A. A., and Wheeler, M. H. (1986) *Annu. Rev. Phytopathol. 24*, 411−451.
2. Howard, R. J., and Ferrari, M. A. (1989) *Exp. Mycol. 13*, 403−418.
3. Chumley, F. G., and Valent, B. (1990) *Mol. Plant-Microbe Interact. 3*, 135−143.
4. Lundqvist, T., Weber, P. C., Hodge, C. N., Braswell, E. H., Rice, J., and Pierce, J. (1993) *J. Mol. Biol. 232*, 999−1002.
5. Lundqvist, T., Rice, J., Hodge, C. N., Basarab, G. S., Pierce, J., and Lindqvist, Y. (1994) *Structure 2*, 937−944.
6. Thompson, J. E., Basarab, G. S., Pierce, J., Hodge, C. N., and Jordan, D. B. (1998) *Anal. Biochem. 256*, 1−6.
7. Thompson, J. E., and Jordan, D. B. (1998) *Anal. Biochem. 256*, 7−13.
8. Kurahashi, Y., Sakawa, S., Kinbara, T., Tanaka, K., and Kagabu, S. (1997) *J. Pestic. Sci. 22*, 108−112.
9. *Agrow* (1997) Vol. 287, pp 21−22, PJP Publications Ltd.
10. Sieverding, E., Hirooka, T., Nishiguchi, T., Yamamoto, Y., Spadafora, V. J., and Hasui, H. (1998) in *Proceedings, The 1998 Brighton Conference*: *Pests and Diseases*, pp 359−366, British Crop Protection Council, Brighton, England.
11. Ou, S. H. (1985) in *Rice Diseases*, 2nd ed., pp 109−201, C. A. B. International, Slough, U.K.
12. Chen, J. M., Xu, S. L., Wawrzak, Z., Basarab, G. S., and Jordan, D. B. (1998) *Biochemistry 37*, 17735−17744.
13. Jordan, D. B., Lessen, T., Wawrzak, Z., Bisaha, J. J., Gehret, T. C., Hansen, S. L., Schwartz, R. S., and Basarab, G. S. (1999) *Biorg. Med. Chem. Lett. 9*, 1607−1612.
14. Basarab, G. S., Jordan, D. B., Gehret, T. C., Schwartz, R. S., and Wawrzak, Z. (1999) *Biorg. Med. Chem. Lett. 9*, 1613−1618.
15. Wawrzak, Z., Sandalova, T., Steffens, J. J., Basarab, G. S., Lundqvist, T., Lindqvist, Y., and Jordan, D. B. (1999) *Proteins: Struct., Funct., Genet. 35*, 425−439.
16. Jordan, D. B., Basarab, G. S., Steffens, J. J., Lundqvist, T., Pfrogner, B. R., Schwartz, R. S., and Wawrzak, Z. (1999) *Pestic. Sci. 55*, 277−280.
17. Basarab, G. S., Steffens, J. J., Wawrzak, Z., Schwartz, R. S., Lundqvist, T., and Jordan, D. B. (1999) *Biochemistry 38*, 6012−6024.
18. Sargent, A. L., Rollog, M. E., Almlof, J. E., Gassman, P. G., and Gerlt, J. A. (1996) *THEOCHEM 388*, 145−159.
19. Gerlt, J. A., and Gassman, P. G. (1993) *J. Am. Chem. Soc. 115*, 11552−11568.
20. Gerlt, J. A., and Gassman, P. G. (1993) *Biochemistry 32*, 11943−11952.
21. Gerlt, J. A., and Gassman, P. G. (1992) *J. Am. Chem. Soc. 114*, 5928−5934.
22. Corey, E. J., and Sneen, R. A. (1956) *J. Am. Chem. Soc. 78*, 6269−6278.
23. Anderson, V. (1998) in *Comprehensive Biological Catalysis*, Vol. 2, pp 115−133, Academic Press, New York.
24. Zheng, Y.-J., and Bruice, T. C. (1998) *Proc. Natl. Acad. Sci. U.S.A. 95*, 4158−4163.
25. Urbauer, J. L., Bradshaw, D. E., and Cleland, W. W. (1998) *Biochemistry 37*, 18026−18031.
26. Northrop, D. B. (1982) *Methods Enzymol. 87*, 607−625.
27. Hanson, K. R., and Rose, I. A. (1975) *Acc. Chem. Res. 8*, 1−10.
28. Wiczoriek, S. J., Kalivoda, K. A., Clifton, J. G., Ringe, D., Petsko, G. A., and Gerlt, J. A. (1999) *J. Am. Chem. Soc. 121*, 4540−4541.
29. Bruice, T. C., and Lightstone, F. C. (1999) *Acc. Chem. Res. 32*, 127−136.
30. Lightstone, F. C., Zheng, Y.-J., and Bruice, T. C. (1998) *J. Am. Chem. Soc. 120*, 5611−5621.

31. Schiott, B., Zheng, Y.-J., and Bruice, T. C. (1998) *J. Am. Chem. Soc. 120*, 7192−7200.
32. Lau, E. Y., and Bruice, T. C. (1998) *J. Am. Chem. Soc. 120*, 12387−12394.
33. Zheng, Y.-J., and Bruice, T. C. (1997) *J. Am. Chem. Soc. 119*, 3868−3877.
34. Zheng, Y.-J., and Bruice, T. C. (1997) *J. Am. Chem. Soc. 119*, 8137−8145.
35. Lightstone, F. C., and Bruice, T. C. (1996) *J. Am. Chem. Soc. 118*, 2595−2605.
36. Ponec, R. (1995) *Top. Curr. Chem. 174*, 1−26.
37. Shin, W., Oh, D.-G., Chae, C.-H., and Yoon, T.-S. (1993) *J. Am. Chem. Soc. 115*, 12238−12250.
38. Hine, J. (1977) *Adv. Phys. Org. Chem. 15*, 1−61.
39. Abell, C. (1998) *Biochem. Soc. Trans. 26*, 310−315.
40. Harris, J. M., Watkins, W. J., Hawkins, A. R., Coggins, J. R., and Abell, C. (1996) *J. Chem. Soc., Perkin Trans. 1 19*, 2371−2377.
41. Chaudhuri, K., Duncan, K., Graham, L. D., and Coggins, J. R. (1991) *Biochem. J. 275*, 1−6.

BI991839Y